THE ASTROPHYSICAL JOURNAL, 322:L15–L20, 1987 November 1

LATE EMISSION FROM SN 1987A

C. FRANSSON
Stockholm Observatory
AND
R. A. CHEVALIER
Department of Astronomy, University of Virginia
Received 1987 June 17; accepted 1987 August 11

ABSTRACT

The early observations of SN 1987A suggest that the progenitor star had an initial mass in the 15–25 $M_\odot$ range and had undergone considerable mass loss. The heavy element mantle gas then has a velocity up to about 2500 km s^{-1}. We model the late emission from the mantle gas under the assumption of energy input by γ-rays from ^{56}Co decays. An emission-line spectrum of low-ionization species is produced at optical through infrared wavelengths. The relative strengths of O I, Si I, and Ca II lines will help to determine the mass of the progenitor star. At an age of $\sim$ 700 days an infrared catastrophe occurs and the gas temperature drops to a few hundred K; most of the radiation is then emitted in infrared fine-structure lines. The γ-ray line intensity peaks in the 15 $M_\odot$ model at an age of 270 days. There is very little production of X-rays below 50 keV if the photon interaction with the hydrogen envelope can be neglected. Radiation from a possible central pulsar nebula will be absorbed by the mantle gas; optical depth unity in the 15 $M_\odot$ model at 10 keV is not reached for 18 yr. If the pulsar nebula radiates most efficiently at X-ray wavelengths, the inner parts of the mantle receive most of the heating, and lines of highly ionized elements in the ultraviolet and optical may be emphasized. The radio emission from the pulsar is likely to be absorbed by the ejecta for several years.

Subject heading: stars: supernovae

I. INTRODUCTION

The small distance to SN 1987A gives us a unique opportunity to study the results of a supernova explosion in detail. This is particularly true for the late epochs when the envelope of the supernova has become transparent to the continuum radiation, and we can study the products of the nucleosynthesis and the effects of a newborn pulsar. Another important advantage is that the physics, in particular the radiative transfer, becomes fairly simple. The fact that the luminosity of SN 1987A increased beginning a few days after the explosion (e.g., Blanco *et al.* 1987) suggests that there is a central energy source that can be expected to excite the central regions of the supernova.

In this *Letter* we examine what multiwavelength observations can tell us about the interior of SN 1987A. McCray, Shull, and Sutherland (1987) have already discussed some of the general effects; here, we use more realistic stellar models and present detailed spectral results. Our models emphasize spectral observations at optical and infrared wavelengths as a means of determining the composition structure of the ejecta. Ultraviolet observations will also be fruitful, but will initially be influenced by line blanketing (Fransson 1987). In a coming paper (Fransson and Chevalier 1987, hereafter Paper II) we will discuss the late emission from supernovae in more detail.

II. NATURE OF THE SUPERNOVA

The important parameters for our study are the composition and density structure of the supernova, the expansion velocity of the core, V_c, the amount of ^{56}Ni initially synthesized in the explosion, M(^{56}Ni), and the properties of a central pulsar and its surrounding nebula. By modeling the light curve of SN 1987A, Woosley, Pinto, and Ensman (1987) find that they get the best agreement during the first month for a 15–20 $M_\odot$ star which has lost most of its hydrogen envelope. Based on the radio observations by Turtle *et al.* (1987) and optical observations, Chevalier and Fransson (1987) also argue that the progenitor of SN 1987A is likely to have been a star of mass $\sim$ 20 $M_\odot$, which has undergone a period of mass loss. From the free-free absorption they derive a mass-loss rate of $\sim 8.8 \times 10^{-6}$ $M_\odot$ yr^{-1}, for a wind velocity of 550 km s^{-1}. On a time scale of $\sim 10^6$ yr most of the hydrogen envelope may thus have been lost. This has the effect that the expansion of the core and mantle will not be slowed down appreciably, as is the case for a star without mass loss. The main difference between the two cases is the much higher velocity of the core region for the star without a massive envelope. For the 4 $M_\odot$ WR model (main-sequence mass 15 $M_\odot$), the velocity of the outer boundary of the oxygen zone is $\sim$ 2430 km s^{-1} (Ensman and Woosley 1987), compared to $\sim$ 900 km s^{-1} for the model with envelope (Weaver and Woosley 1980). In both cases the density at the O/He interface shows a large drop, reflecting the structure of the progenitor.

Although the mass is probably constrained to be in the range 15–25 $M_\odot$, this uncertainty is very important for the nucleosynthesis (Woosley and Weaver 1987). The total mass

of elements heavier than helium increases from 1.06 $M_\odot$ to 3.80 $M_\odot$ in this range. We have therefore calculated one set of models with a main-sequence mass of 15 $M_\odot$ and one with 25 $M_\odot$. For the core structure we have used the Ensman and Woosley (1987) models 4A and 8A. The results are sensitive to the density distribution and core velocity. For a realistic comparison, these quantities should be obtained from the observed line profiles. At the epochs of interest, the velocity field has relaxed to a $V \propto r$ law. For an optically thin line the emission per volume, $j(r)$, is related to the intensity, $I(\varepsilon)$, of the line at the dimensionless frequency ε by

$$j(r = \varepsilon R) = \frac{1}{2\pi\varepsilon R^2}\frac{dI(\varepsilon)}{d\varepsilon}.$$

Here $\varepsilon = (1 - \nu/\nu_0)c/V_0$, and ν and ν_0 the frequency and the rest frequency of the line, respectively; R, the maximum radius of the supernova; and V_0, the velocity at this point. One can thus from the observed line profile determine the emissivity as a function of the radius εR, and thus the γ-ray input and density. This relation is valid for an optically thin line, like the forbidden [O I] $\lambda\lambda$6300–64 lines. For thick lines, j is replaced by the source function.

Hydrodynamic models (Ensman and Woosley 1987) predict that the O region should be a geometrically thin shell, giving a flat profile. The observations of SN 1985F, on the other hand, are more compatible with a centrally peaked density distribution (Fransson 1986; Paper II). Hydrodynamic instabilities during the first days may lead to mixing between different burning shells. If clumps of the dense core material penetrate into the He and H envelopes, the line profiles of the metal lines will extend to higher velocities. Observations of Cas A (Chevalier and Kirshner 1979) show evidence for this type of mixing.

In the 15 $M_\odot$ and 25 $M_\odot$ models studied here, the mass of ^{56}Ni was 0.10 $M_\odot$ and 0.28 $M_\odot$, respectively. The γ-ray luminosity is $L_\gamma = 1.36 \times 10^{42}\ [M(^{56}\mathrm{Ni})/0.1\ M_\odot] \exp(-t/114\ \mathrm{days})$ ergs s^{-1}. At an age of 86 days, SN 1987A had a magnitude $V = 3.0$ (Hamuy and Phillips 1987). If the conversion to total luminosity was similar to that at earlier times (Blanco *et al.* 1987) and radioactivity was the primary energy source, the luminosity was 9×10^{41} ergs s^{-1} and the ^{56}Ni mass was 0.11 $M_\odot$ (see also Gehrels, MacCallum, and Leventhal 1987). In our modeling, we have emphasized energy input from radioactive decays of ^{56}Co because the amount synthesized is fairly well determined by theoretical calculations and because there is observational evidence for this heat source in the explosions of massive stars (Barbon, Cappelaro, and Turatto 1984; Wheeler and Levreault 1985).

III. RADIOACTIVE ENERGY INPUT

The γ-ray lines emitted by ^{56}Co decays, in the 0.51–3.26 MeV range, interact with the supernova through Compton scattering and photoelectric absorption. Both for the heat input and for the observability of the X-ray emission we are interested in the X-ray absorption of the ejecta. Including all interesting elements with K-shell cross sections from Reilman and Manson (1979), we have calculated the absorption optical depth to the X-rays for the Ensman and Woosley (1987) model 4A (ZAMS mass 15 $M_\odot$), with $V_c = 2430$ km s^{-1}. The optical depth 300 days after the explosion is shown in Figure 1, and scales as $(V_c t)^{-2}$. Due to the low density, the extended He envelope contributes negligibly to the column density. The same is true for a H envelope. Most of the absorption below 7 keV is due to the O and Si-Ca regions. In the former, O dominates the absorption, and in the latter region S and Si contribute equal amounts. The internal absorption by the Fe-Co core depends sensitively on the extent of the core, or equivalently on its density. In the models by Ensman and Woosley, the radioactive heating of the central parts leads to a low-density Fe-Co region, and consequently only displayed a weak Fe edge at 7.0 keV. The X-ray opacity above 7 keV for this composition is 97 $(E/7\ \mathrm{keV})^{-2.8}$ cm^2 g^{-1}. A model with constant density inside the He/O interface gave an absorption at the Fe edge a factor of 2.1 stronger than this model, while the 8A model (ZAMS mass 25 $M_\odot$) gave a factor 2.2 higher optical depth compared to model 4A, mainly due to the larger core mass. The energy corresponding to absorption optical depth unity of the ejecta can be well represented by the formula

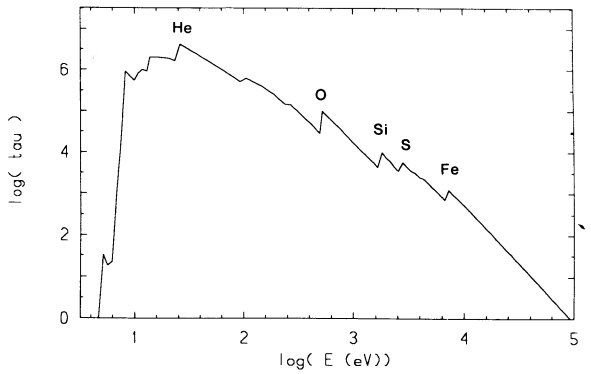

FIG. 1.—Optical depth of the Ensman-Woosley model 4A, with $V_c = 2430$ km s^{-1}, in the range 0.01–100 keV 300 days after the explosion. For other epochs and core velocities $\tau(E)$ scales as $(V_c t)^{-2}$.

$$E(\tau = 1) = 81(M_c/1\ M_\odot)^{0.36} \times (V_c/2500\ \mathrm{km\ s^{-1}})^{-0.72} t_{\mathrm{year}}^{-0.72}\ \mathrm{keV},$$

where M_c is the mass inside the O/He interface, 1.0 $M_\odot$ for model 4A and 2.6 $M_\odot$ for model 8A. For O and Si, Compton scattering becomes important above 28 keV, and 50 keV, respectively. For Fe, photoabsorption dominates for energies less than $\sim$ 100 keV. These are thus the energies where the down-scattered γ-rays from the ^{56}Co will be absorbed by the gas.

For the 1.0 $M_\odot$ core mass of model 4A, we have calculated the escape and Compton degradation of the ^{56}Co γ-rays. We include angle-dependent Compton scattering and photoelectric absorption in a Monte Carlo calculation; this is similar to calculations by Gehrels, MacCallum, and Leventhal (1987) (see also Woosley, Pinto, and Ensman 1987). The core is modeled in a one-zone approximation, with constant density and total absorption given by the above values (see Fig. 1). The 0.847 MeV γ-ray line emission rises rapidly at $\sim$ 90 days

and peaks at a relatively early time, 270 days, as expected for a low-mass core with a relatively large velocity. The peak flux was 2.8×10^{-2} photons cm^{-2} s, for $M(^{56}\mathrm{Ni}) = 0.1\ M_\odot$. The 100–200 keV continuum peaked at $\sim$ 180 days with a flux of 3.0×10^{-2} photons cm^{-2} s^{-1}. The X-ray flux in the 50–75 keV band is low as a result of absorption by Fe and there is little X-ray emission below 50 keV.

As noted by Gehrels, MacCallum, and Leventhal (1987), the production of lower energy X-rays depends on the amount of Compton scattering in the hydrogen-rich gas. Due to the smaller metal abundance, X-rays produced here suffer less from the photoelectric absorption. In our model, we have assumed that this is negligible so that a minimum amount of X-rays is produced.

The γ-ray photons from ^{56}Co have an effective opacity for energy deposition of ~ 0.03 cm^2 g^{-1}. Once the γ-ray optical depth, $\tau_\gamma \approx 3.1\ (M_c/M_\odot)(V_c/2500\ \mathrm{km\ s^{-1}})^{-2}(t/100\ \mathrm{days})^{-2}$, becomes less than unity the energy input per unit mass will be evenly distributed. The MeV γ-rays lose most of their energy by inelastic Compton scattering. The resulting nonthermal electrons are then slowed down by ionizations, excitations and heating of the thermal, free electrons. We have performed Monte Carlo calculations showing that for an electron fraction, x_e, larger than 0.1, relevant during the first $\sim$ 300 days, excitation to discrete states can be neglected. The energy going into ionizations will emerge mainly as recombination emission, whereas that going into heating will be balanced by collisional excitations of low forbidden and semiforbidden transitions.

To model the expected emission from SN 1987A, and to show the diagnostic potential of late-type observations, we have calculated the conversion of the high-energy radiation into UV, optical, and IR emission. The degradation of the γ-rays by Compton scatterings, and subsequent ionizations and heating of the gas are calculated by a Monte Carlo method. These results are combined with a calculation of the ionization balance and the temperature of the ejecta. As input, we use the explosion models by Ensman and Woosley (1987) and Woosley and Weaver (1987). The elements included were He, C, O, Ne, Na, Mg, Si, S, Ar, Ca, and Fe. For O I and Ca II the lowest nine and four energy levels, respectively, were taken into account. Permitted and semiforbidden lines were calculated as two-level atoms, and for the forbidden lines we solved for the three lowest levels. For iron we have used the results of Axelrod (1980), which give the correct total cooling, but no details of the emitted spectrum. This is reasonable for massive cores without strong mixing, since other elements, in particular oxygen, dominate the abundance of iron. Hydrogen was not included, since it should be physically separated from the more advanced burning stages unless complete mixing occurs. The atomic data used in the calculations were taken from the most recent calculations (e.g., the compilation by Mendoza 1983; Paper II).

In Figure 2 we show the resulting luminosities in the various lines per unit mass through the ejecta for the 8A, 25 $M_\odot$ model with $V_c = 2600$ km s^{-1}, 300 days after the explosion. Comparing this with the abundance structure in Woosley and Weaver (1987), it is seen that the emission qualitatively resembles the shell structure of the supernova.

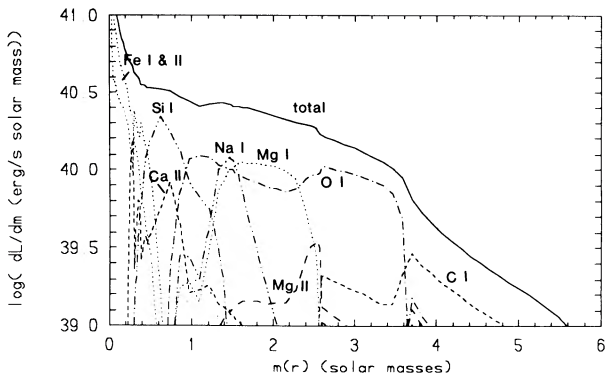

FIG. 2.—Luminosity per unit mass of the most important lines 300 days after the explosion for the 8A model (ZAMS 25 $M_\odot$). The velocity at the O/He interface was 2600 km s^{-1}.

The total flux of radiation coming from the various shells depends on the γ-ray heat input, which is proportional to $\Delta\tau_\gamma \approx 0.03\rho\ \Delta r$, where Δr is the shell thickness and ρ the density. In principle, the line profiles can give direct information about these quantities (§ II). *Within* a given zone, the line strengths depend on the composition, and the ionization and temperature of the gas. Thus the Si-Ca zone is characterized by strong emission in Ca II] λ7300, the 8498–8662 triplet and the [Si I] 1.091 μm and 1.6068–1.6455 μm lines. Even though O dominates the abundance of Mg by a factor of $\sim$ 15 in the inner part of the O zone, Mg I] λ4571 and Na I λλ5890–96 have comparable strengths to the [O I] λλ6300–64 lines. The high density of the core results in a large neutral fraction of Mg and Na, explaining their strengths. In the outer O zone ^{24}Mg drops by a factor $\sim$ 30, and [C I] λ8729 becomes the next strongest line after the [O I] line. Finally, in the He shell the He I recombination lines, most notably the 5876 Å line, are weak since only $\sim$ 2% of the total ionization energy into He is emitted in this transition. Instead, most of the cooling is controlled by [C I] λ8727. The He zone may thus be observed as an extended, weak high-velocity wing of this line. At 300 days the temperatures of the various zones are $\sim$ 4000 K for the Si-Ca shell, $\sim$ 4500–5000 K for the O shell, and $\sim$ 5800–7000 K for the He shell. The electron fraction decreases from $\sim$ 0.3 close to the center to $\sim$ 0.1 in the He shell.

The resulting spectrum in the optical region 300 days after the explosion for the 25 $M_\odot$ model is shown in Figure 3. The large mass and corresponding column density of the oxygen shell for the 25 $M_\odot$ star is reflected in the large luminosity in the [O I] λλ6300–64 lines, being the characteristic of stars in this mass range and higher. In Table 1 we give the fluxes of the other strong lines relative to the [O I] λλ6300–64 lines. The Na I, Mg I], and [Si I] lines are rather uncertain, since they are sensitive to the ionization equilibrium, and thus density, and for [Si I] to uncertain collision data. As a comparison we have also calculated a 15 $M_\odot$ model from Woosley and Weaver (1987), scaled in velocity to $V_c = 1200$ km s^{-1}, also given in Table 1. The lower core velocity is consistent with the Woosley, Pinto, and Ensman (1987) 15B

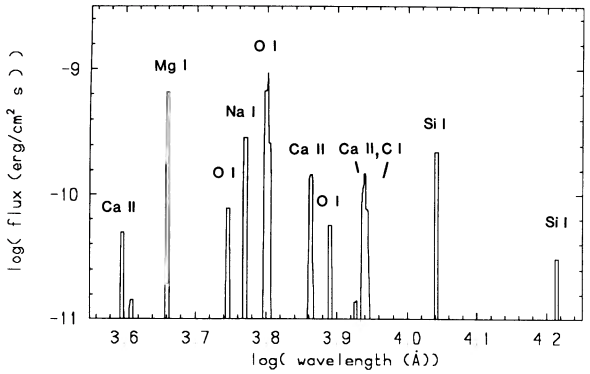

FIG. 3.—Synthetic spectrum for the 8A (ZAMS 25 $M_\odot$) model with V_c = 2600 km s^{-1} at 300 days. Note that several lines are blends (Table 1).

TABLE 1

LUMINOSITIES RELATIVE TO [O I] λλ6300–64 OF THE STRONGEST LINES FOR THE 25 $M_\odot$ AND 15 $M_\odot$ MODELS AT 300 DAYS

PARAMETER	ZAMS MASS ($M_\odot$)	
	25	15
V_c (km s^{-1})	2640	1200
$M(^{56}\mathrm{Ni})$ ($M_\odot$)	0.28	0.10
L(6300–64) (er s^{-1})	2.38×10^{40}	3.32×10^{39}
[C I] 8727	0.21	0.52
O I 1356	0.10	0.11
[O I] 5577	0.015	0.42
[O I] 6300–64	1.0	1.0
O I 7774	0.09	0.21
Na I 5890–96	0.31	0.47
Mg I] 4571	0.63	1.43
Mg II 2800	0.25	0.30
[Si I] 10991	0.08	0.93
[Si I] 16455	0.02	0.30
[S II] 4069–76	0.00	0.63
[S II] 10286	0.00	0.33
Ca II 3934–68	0.04	0.70
Ca II] 7291–7332	0.11	1.58
Ca II 8498–8662	0.09	1.27

NOTE.—L (6300–64) is the absolute luminosity of the [O I] λλ6300–64 line.

model for SN 1987A. The 15 $M_\odot$ spectrum differs mainly from the 25 $M_\odot$, in that the Ca II and [Si I] IR lines are much stronger relative to the [O I] lines. The reason for the large Ca II strengths can be traced to the different Ca/O ratios, 0.10 in the 15 $M_\odot$ star, and 0.0082 in the 25 $M_\odot$ star (Woosley and Weaver 1987). Further, in the 15 $M_\odot$ model, Ca and O are mixed in most of the core, whereas in the 25 $M_\odot$ model they occur in separate regions. Due to the efficient cooling of Ca II compared to [O I], Ca II dominates the emission in most of the core, in spite of its smaller abundance. The same explanation applies to [Si I]. The mixing of Si-Ca in the O shell is, however, sensitive to the treatment of the convection (Woosley, Pinto, and Ensman 1987) as well as instabilities. The Ca II]/[O I] ratio varies also with the core density, and thus V_c. The unscaled 4A model with V_c = 2430 km s^{-1} had a Ca II]/[O I] ratio of ~ 5.6 at the same epoch. Even with these caveats, we expect the Ca II/[O I] ratio to be a good diagnostic of the core mass.

The time evolution of the spectrum is governed by the decaying γ-ray luminosity and the expansion of the ejecta. The most interesting aspect is the sudden transition from a spectrum dominated by optical lines to a spectrum dominated by IR and far-IR lines. Because of the decreasing γ-ray input, the heating per volume decreases faster than the radiative cooling, and the temperature falls gradually. Adiabatic cooling is, however, unimportant. When the temperature is 2000–3000 K the cooling becomes dominated by IR fine-structure lines, in particular [O I] 63.15 μm. Since the excitation temperatures are typically ~ 300 K, the temperature must fall to a value of this order to balance the heating. This has the character of a thermal instability, and is similar to the "IR-catastrophe" found for a Fe-Co plasma by Axelrod (1980). The exact epoch when this occurs is set by the time when the γ-ray ionization parameter, $\Gamma_\gamma = L_\gamma/4\pi r^2 cn\chi$, is in the range 0.1–1, depending on the density (Fransson 1986). Here n is the total density and χ is the γ-ray energy needed for each ionization, ~ 30 eV for oxygen.

We have calculated the spectral evolution for the 4A = 15 $M_\odot$ and 8A = 25 $M_\odot$ models, with V_c = 1200 and 2600 km s^{-1}, respectively, from 200 up to 800 days. In Figure 4 the luminosities in the most important lines are shown for the scaled 4A model with V_c = 1200 km s^{-1} and $M(^{56}\mathrm{Ni})$ = 0.1 $M_\odot$. Since the total absorbed γ-ray energy is proportional to $t^{-2}\exp(-t/114)$, we factor out this dependence and define "scaled" line luminosities, l, by $l(t) = L(t)\,(t/300)^2 \exp[(t - 300)/114]$. Between 200 and 300 days Mg I] λ4571 is the strongest line after which Ca II] λ7300 together with [Si I] 1.099 μm, 1.645 μm dominate up to 600 days. Finally, at 600 days the transition to the fine-structure lines, with [O I] 63.15 μm and [S I] 25.25 μm as the strongest, occur. Both the [Si I] and [S I] lines are however, sensitive to the assumptions about convective mixing in the core. A similar plot for the 25 $M_\odot$ model showed a dominance of [O I] λλ6300–64 and 63.15 μm

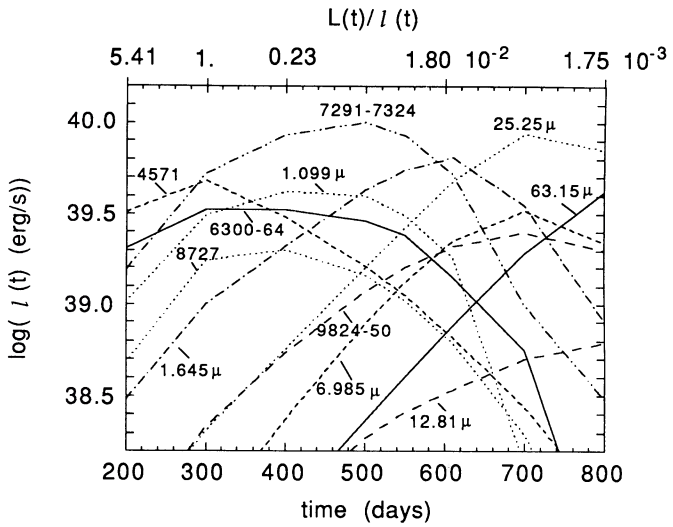

FIG. 4.—Line luminosities as a function of time for model 4A (ZAMS 15 $M_\odot$), with V_c = 1200 km s^{-1} and $M(^{56}\mathrm{Ni})$ = 0.1 $M_\odot$. The "scaled" line luminosity, l, is related to the luminosity L by $l(t) = L(t)\,(t/300)^2 \exp[(t - 300)/114]$. For convenience, the conversion factor $L(t)/l(t)$ is given on top of the figure for a few dates. For identification of the lines, see Table 1 and text.

over the rest of the lines throughout the whole evolution. The transition to the IR-dominated spectrum occurred for both masses at ~ 700 days. In these calculations direct excitations to discrete levels by the fast electrons are not included. Although nearly all the γ-ray heating leads to IR lines, the direct excitations and the recombination emission can lead to an observable flux in the UV and optical lines at late times. For O we find that for $x_e = 10^{-2}$, ~ 5% of the energy results in direct excitations, compared to ~ 42% in heating of the electrons. Most of this goes into the [O I] λλ6300–64 and O I λ1302 *N*S6 lines. At 900 days the temperature of the ejecta was ~ 600 K in the O zone and even lower in the Si-Ca region, ~ 300 K. Because of the low metal abundance in the He shell the temperature was much higher, ~ 2600 K, with most of the emission due to[C I] λλ9824–50.

At these late stages the different compositions are reflected in, e.g., the [O I] 63.15 μm/[S I] 25.25 μm ratio. At 750 days we find the following fluxes (in ergs cm^{-2} s^{-1}) for the 8A model: [O I] 63.15 μm, 4.1×10^{-10}, [Ne II] 12.81 μm, 7.6×10^{-11}, [Si I] 1.645 μm, 8.3×10^{-11}, [Si I] 68.49 μm, 1.7×10^{-11}, [S I] 25.25 μm, 5.1×10^{-11}, and [Ar II] 6.985 μm, 1.6×10^{-11}. At the same epoch the 4A model with $V_c = 1200$ km s^{-1} (Fig. 4) gave the following fluxes for the same lines: 6.2×10^{-11}, 1.3×10^{-11}, 3.0×10^{-11}, 1.3×10^{-11}, 1.8×10^{-10}, and 6.5×10^{-11}. The fluxes in most of these lines are considerably higher at earlier epochs (Fig. 4) and are thus important to monitor. Since the electron densities are likely to be larger than ~ 10^5 cm^{-3}, most fine-structure lines will be in LTE and the fluxes therefore a direct measure of the mass of the different elements.

We note that at the time of the infrared catastrophe, the gas temperature drops to the point where dust and molecule formation may become possible.

IV. A CENTRAL PULSAR

We expect that radioactive energy input is likely to dominate the initial emission from SN 1987A after it becomes optically thin. However, energy from a central pulsar has a long decay time and may eventually dominate the emission properties. The pulsar loses most of its rotational energy, L_p, in the form of a wind of relativistic particles and magnetic flux. Part of the energy will be emitted directly, probably mainly as X-rays. The expanding bubble of relativistic particles will also interact with the slow-moving ejecta, giving rise to an expanding shock wave radiating its energy as soft X-rays (Chevalier 1977). About 0.03 of L_p is radiated in this way. For a core mass M_c (in solar masses), expanding with velocity $V_c r/R_c$, the temperature behind the shock will be $T_s = 2.2 \times 10^5 (V_c/1000 \text{ km s}^{-1})^{6/5} (L_p/10^{40} \text{ ergs s}^{-1})^{2/5} M_c^{-2/5} (t/100 \text{ days})^{2/5}$ K, assuming the gas to have $A/Z \approx 2$. For a pulsar luminosity of 10^{40} ergs s^{-1} we get $T_s = 1.1 \times 10^6$ K for the 15 $M_\odot$ model with $V_c = 2430$ km s^{-1}, 1 year after the explosion. The observability of this radiation will therefore be difficult, because of the absorption of the ejecta and the intersteilar gas.

The large optical depth during the first years at keV energies (Fig. 1) means that the X-ray input to the ejecta, and thus the line emission, will be sensitive to the spectral shape of the emission from the pulsar. In contrast to the γ-ray heated case only the very central parts close to the pulsar nebula will be heated during the first year. The situation will thus be that of a photoionized gas, with a high temperature, $(1–3) \times 10^4$ K, and high ionization close to the boundary. Most of EUV and soft X-ray flux will be absorbed here and emerge as ultroviolet lines of ions like C III–IV, O III–IV, Si III–IV, and Fe III–IV. The exact line spectrum is sensitive to the structure close to the bubble boundary. Further out, lines of O II, Ca II, and Si I should be prominent.

Absorption by the mantle gas is an impediment to observing the pulsar nebula directly. In model 4A with $V_c = 2430$ km s^{-1}, we estimate that optical depth unity at 10 keV is reached at an age of 18 yr. The radio emission from a pulsar will be strongly absorbed by free-free absorption in the ejecta. Assuming that the ionization is dominated by the γ-rays we find that the optical depth at a wavelength λ is given by

$$\tau_{\rm ff} = 2.7 \times 10^{-15} \lambda^2 L_\gamma \int_{R_{\rm in}} \frac{\rho(r)}{\alpha_r r^2 T(r)^{1.5}}\, dr,$$

where α is the recombination coefficient. Therefore $\tau_{\rm ff}$ is set by the density, ρ, and temperature, T, close to the pulsar bubble-ejecta interface. For the uniform density core, discussed earlier, we have $R_{\rm in} = 1.4 \times 10^{15}$ $(V_c/1000$ km $s^{-1})^{3/5} (L_p/10^{40}$ ergs $s^{-1})^{1/5} M_c^{-1/5} t_{\rm yr}^{6/5}$ cm. Assuming the core to be dominated by oxygen we find

$$\tau_{\rm ff} = 1.3 \times 10^3 \lambda^2 \left[M(^{56}\text{Ni})/0.1 \right] e^{-t/114 \text{ days}} \times M_c \left(V_c/1000 \text{ km s}^{-1} \right)^{-3} \left(t/1000 \text{ days} \right)^{-3} \times \left(T/10^4 \text{ K} \right)^{-0.75} \left(R_{\rm in}/10^{15} \text{ cm} \right)^{-1}.$$

Setting all parameters in parentheses equal to one, we find that unity depth is reached after ~ 2 yr at 1 cm, for $M_c = 1\ M_\odot$.

In the same way, if the pulsar nebula emits an ionizing spectrum with power-law index α and luminosity L_i above 13.6 eV, we find that $\tau_{\rm ff} \approx 1$ corresponds to a time

$$t(\tau_{\rm ff} = 1) = 13.1 \lambda^{5/6} (1 - 1/\alpha)^{5/12} \left(L_i/10^{40} \text{ ergs s}^{-1} \right)^{5/12} \times \left(L_p/10^{40} \text{ ergs s}^{-1} \right)^{-1/6} \left(V_c/1000 \text{ km s}^{-1} \right)^{-1/2} \times M_c^{1/6} \left(T/10^4 \text{ K} \right)^{-0.32} \text{ yr}.$$

Thus, for typical parameters the optical depth will be large for several years. These time scales are, however, reduced if the nebula sweeps up the supernova gas and it fragments into filaments (Chevalier 1977; Bandiera, Pacini, and Salvati 1983).

We are grateful to L. Ensman and S. Woosley for providing us with detailed stellar models, and to many authors for sending their preprints on SN 1987A. R. A. C.'s research is supported in part by NSF grant AST-8615555 and by NASA grant NAGW-764.

REFERENCES

Axelrod, T. S. 1980, Ph.D. thesis, University of California, Santa Cruz.
Bandiera, R., Pacini, F., and Salvati, M. 1983, *Astr. Ap.*, **126**, 7.
Barbon, R., Cappelaro, E., and Turatto, M. 1984, *Astr. Ap.*, **135**, 27.
Blanco, V. M., *et al.* 1987, *Ap. J.*, **320**, 589.
Chevalier, R. A. 1977, in *Supernovae*, ed. D. N. Schramm (Dordrecht: Reidel), p. 53.
Chevalier, R. A., and Fransson, C. 1987, *Nature*, **328**, 44.
Chevalier, R. A., and Kirshner, R. P. 1979, *Ap. J.*, **233**, 154.
Ensman, L., and Woosley, S. E. 1987, in preparation.
Fransson, C. 1986, *Highlights Astr.*, **7**, 611.
_____. 1987, in *Proc. of the ESO Workshop on SN 1987A*, ed. I. J. Danziger, in press.
Fransson, C., and Chevalier, R. A. 1987, in preparation (Paper II).
Gehrels, N., MacCallum, C. J., and Leventhal, M. 1987, *Ap. J. (Letters)*, **320**, L19.
Hamuy, M. and Phillips, M. M. 1987, *IAU Circ.*, 3498.
McCray, R., Shull, J. M., and Sutherland, P. 1987, *Ap. J. (Letters)*, **317**, L73.
Mendoza, C. 1983, in *IAU Symposium 103, Planetary Nebulae*, ed. D. R. Flower (Dordrecht: Reidel), p. 143.
Reilman, R. F., and Manson, S. T. 1979, *Ap. J. Suppl.*, **40**, 815.
Turtle, A. J., *et al.* 1987, *Nature*, **327**, 38.
Weaver, T. A., and Woosley, S. E. 1980 in *Supernova Spectra*, ed. R. Meyerott and G. H. Gillespie (New York: AIP), p. 15.
Wheeler, J. C., and Levreault, R. 1985, *Ap. J. (Letters)*, **294**, L17.
Woosley, S. E., Pinto, P. A., and Ensman, L. 1987, *Ap. J.*, in press.
Woosley, S. E., and Weaver, T. A. 1987, preprint

ROGER A. CHEVALIER: Department of Astronomy, University of Virginia, PO Box 3818, Charlottesville, VA 22903.

CLAES FRANSSON: Stockholm Observatory, S-133 00 Saltsjöbaden, Sweden